Copolymerization of Cyclic Phosphonate and Lactide: Synthetic Strategies towards Control of Amphiphilic Microstructure

James Beament,[§] Thomas Wolf,[‡] Jens C. Markwart,[‡] Frederik R. Wurm,[‡] Matthew D. Jones[§*] and Antoine Buchard[§*]*

[§] Department of Chemistry, University of Bath, Claverton Down, Bath BA2 7AY, U. K.

[‡] Max Planck Institute for Polymer Research, Ackermannweg 10, D-55128 Mainz, Germany

For Table of content use only:

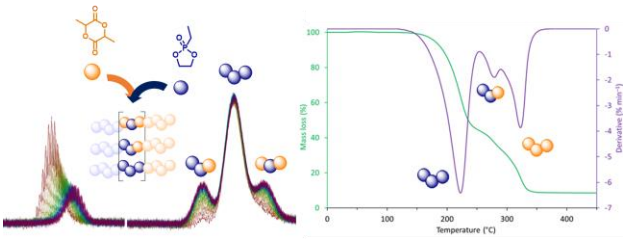

ABSTRACT: Controlling the microstructure of polymers through chemical reactivity is key to control the material properties of synthetic polymers. Herein, we investigate the ring-opening copolymerization of a mixture of lactide and 2-ethyl-2-oxo-1,3,2-dioxaphospholane, promoted by an aluminum pyrrolidine monophenolate complex or 1,8-diazabicyclo[5.4.0]undec-7-ene (DBU). This monomer mixture provides fast access to amphiphilic copolymers. The reaction conditions

control the copolymer microstructure, which has been determined via a combination of ^{1}H and ^{31}P NMR spectroscopy. The choice of initiator has a profound impact: both initiators produce tapered block copolymers, but with reverse monomer selectivity. While the aluminum initiator favors the cyclic phosphonate monomer, DBU favors lactide polymerization. Moreover, a sequential control of temperature facilitates the preparation of block copolymers in one-pot. Thermal properties measured by TGA and DSC correlate to copolymer architectures. This methodology is the first report of copolymerization between cyclic phosphonates and lactide, and opens the possibility to tune the thermal properties, solubility and degradation rates of the resulting materials.

INTRODUCTION

Poly(lactic acid) (PLA) is arguably one of the most promising commodity plastics, derived from renewable feedstock and industrially compostable, which has penetrated a highly unsustainable market of non-degradable polymers based around crude-oil feedstocks.[1–3] The production of PLA was close to 220 000 tonnes in 2017 and is predicted to increase by 50% by 2022.[4] Much research has been directed towards improving the thermal properties of PLA, in particular through the development of stereoselective ring-opening polymerization (ROP) catalysts for lactide.[5] In parallel, increasing efforts have focused on improving the biodegradability of PLA and its composites in natural and landfill environments.[6–8] Notable strategies have included the development of PLA-based polymer blends,[9–14] as well as copolymerization methods to incorporate more degradable linkages into the PLA polyester backbone.[15,16]

In that regard, phosphorus(V) based monomers, such as phosphoesters {P(=O)$(OR)_2$OR'}, phostones or phosphonates {P(=O)$(OR)_2$R'} are of interest due to their low toxicity and facile hydrolysis. Furthermore, whilst they have been polymerized via step-growth esterification and

acyclic diene metathesis,[17,18] cyclic phosphoesters, phostones and phosphonates are also amenable to ROP,[19,20] which allows copolymerization with lactide.

Penczek and coworkers first investigated polyphosphoesters (–[P(=O)(OR')ORO]$_n$–) in 1976, as precursors for polyelectrolytes.[21] Since then, these polymers and related polyphosphates have been widely studied for biomedical applications and as flame retardants.[20,22–24] Catalytic ROP of five-membered cyclic phosphoesters has been demonstrated to produce well-defined polyphosphoesters,[25,26] with recent catalyst development (*e.g.* the combination of thioureas (TUs) and 1,8-Diazabicyclo[5.4.0]undec-7-ene (DBU))[27–30] overcoming the broad molecular weight distributions from initial studies.[31–36] Block copolymers of cyclic phosphoesters and lactide synthesized via sequential addition have been studied and applied for tissue engineering and drug delivery, [37–40] these systems showing high rates of enzymatic degradation under physiological conditions.[37]

Polyphosphonates (–[P(=O)R'ORO]$_n$–) are another class of phosphorus(V) based polymers which differ from polyphosphates in their alkyl side arm (R'), which alters polymerization kinetics and degradation rates compared to phosphates analogs.[41–43] Wurm and coworkers have thus recently synthesized copolymers of phosphonates (PPn) with hydrophilic and hydrophobic segments, which have both lower and upper critical solution temperatures, yielding a route to self-assembled and degradable polymersomes.[44] Compared to polyphosphates, polyphosphonates are less susceptible to transesterification, so that simple ROP initiating systems such as DBU/alcohol can be used in a controlled manner with cyclic phosphonates. A few metal catalytic systems have also been reported, with comparable control and faster rates than organocatalysts.[36,45] As polyphosphonates give fast access to hydrophilic and low-T_g polymers with a low tendency towards transesterification, copolymerization with lactide would be a straightforward way to

amphiphilic PLA-derivatives with adjustable thermal properties. The variety of catalytic strategies that have been developed for lactide ROP could further enable the control of the comonomers reactivity and the production of polyesters with defined sequence and enhanced, tailored degradability. However, to date copolymers of cyclic phosphonates and lactide have not been investigated.

Herein, we have explored the formation of copolymers of rac-LA and L-LA with 2-ethyl-2-oxo-1,3,2-dioxaphospholane (EtPPn) using a pyrrolidine salan Al complex or DBU (see Figure 1). We have investigated the influence of the catalyst on the copolymerization kinetics and copolymer microstructure. We also report how a temperature switch can be exploited in combination with the Al system to control comonomer reactivity and prepare, in one pot, PLA-EtPPn block copolymers. We have investigated how the different initiators and polymerization conditions affect the thermal properties (in particular the T_g) of the resulting copolymer.

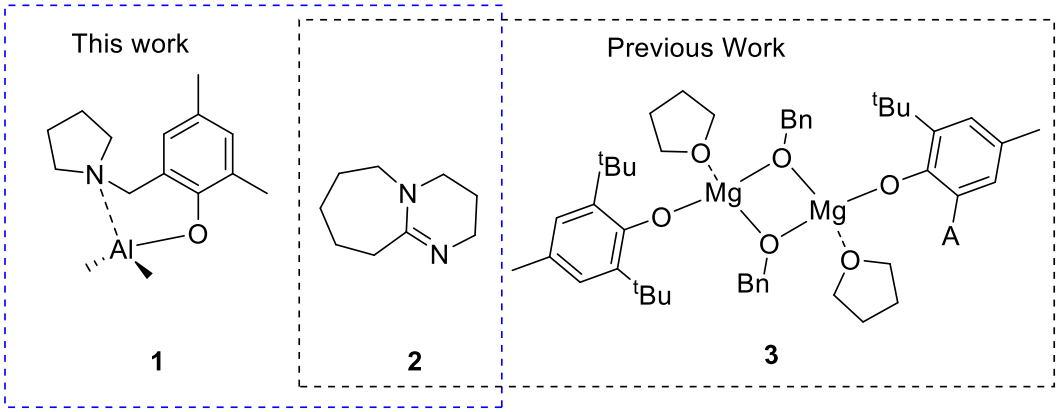

Figure 1. Initiators for the ROP of EtPPn.

RESULTS AND DISCUSSION

Homopolymerization of EtPPn. To date EtPPn has only been polymerized with a few catalytic systems (Figure 1 and Table 1, entries 7-8). We first tested its polymerization with Al pyrrolidine complex **1** in the presence of benzyl alcohol (BnOH) as co-initiator, a system that we have recently

reported for the ROP of lactide.[46] Initiator **1** was active at both 25 °C and 80 °C for the ROP of EtPPn. Under solvent free conditions, at 25 °C and a $[EtPPn]_0$:$[\mathbf{1}]_0$:$[BnOH]_0$ feed ratio of 50:1:1 ($[\mathbf{1}]_0$ = 0.86 mol L^{-1}), 90% monomer conversion was observed within 5 minutes, with excellent control of the molecular weight (Table 1, entry 1). Reactions under dilute conditions ($[EtPPn]_0$ = 0.35 mol L^{-1}), in either CH_2Cl_2 or toluene, maintained good conversion (89-96%), albeit after longer reaction times (Table 1, entries 2-3). Furthermore, increasing initial monomer concentration from 0.35 to 0.7 mol L^{-1} increased conversion (Table 1, Entry 3-6).

Table 1. Ring-Opening Polymerization of EtPPn[a]

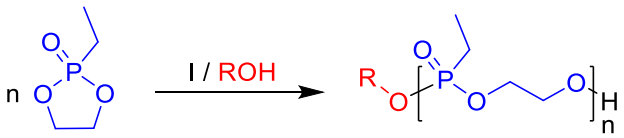

Entry	I	T (°C)	Solvent	Time (h)	[EtPPn] (mol L^{-1})	Conv (%)[c]	M_n^{theo} (kg mol^{-1})[d]	M_n^{SEC} (kg mol^{-1}) [$Đ$][e]
1	**1**	25	N/A	0.08	Bulk	90	6.2	4.3 [1.11]
2	**1**	25	DCM	3	0.35	96	6.6	5.3 [1.14]
3	**1**	25	Tol	24	0.35	89	6.2	4.9 [1.32]
4	**1**	80	Tol	4	0.35	55	3.8	3.1 [1.20]
5	**1**	25	Tol	24	0.7	99	6.8	4.8 [1.38]
6	**1**	80	Tol	4	0.7	90	6.2	5.3 [1.21]
7	**2**[41]	25	DCM	16	4	90	6.2	5.4 [1.07]
8[b]	**3**	–20	THF	1	2	89	12.2	14.2 [1.46]

[a] I: Initiator, $[EtPPn]_0$:$[I]_0$:$[BnOH]_0$ = 50:1:1; [b] $[EtPPn]_0$:$[\mathbf{3}]_0$ = 100:1, **3** = $[(BHT)Mg(OBn)(THF)]_2$;[36] [c] Conversion calculated from ^1H NMR by relative integration of the CH_2 signals in the polymer (1.74 – 1.85 ppm) and in the monomer (1.93 – 2.03 ppm); [d] [((Conversion [M]/100 × $[M]_0$:$[I]_0$) × 136.03) + 108]; [e] Determined by SEC in DMF at 60 °C.

Sequential polymerization of EtPPn and lactide. Copolymerization of L-lactide (L-LA) and EtPPn was next investigated using **1** in toluene with a total monomer concentration of 0.7 mol L^{-1}. Initially, sequential addition of monomers was investigated to produce block copolymer. Complete conversion of L-LA (96%) with **1** was found to require 24 hours at 80 °C (for $[LA]_0$ = 0.35 mol L^{-1} and $[LA]_0$:$[I]_0$:$[BnOH]_0$ = 50:1:1). Cooling down the active solution to 25 °C followed by addition of 50 equivalents of EtPPn (0.35 mol L^{-1}) yielded high conversions of EtPPn after one hour (88%). Conversions of both monomers were determined by relative integration of polymer signals in the ^{1}H NMR spectra of the crude reaction mixture (following quenching). Relative integration of the ^{31}P NMR spectra further confirmed EtPPn conversions.

^{1}H and ^{31}P DOSY NMR experiments indicated only one diffusing polymer species (Figures S8 and S16), supporting the formation of a copolymer. Size-exclusion chromatography (SEC) also revealed a unimodal trace, with molecular weights in good agreement with expected values (M_n^{theo} = 13.0 kg mol^{-1}, M_n^{SEC} = 10.5 kg mol^{-1}). Insight into the poly(phosphonate-*b*-lactide) chain microstructure was determined via ^{31}P NMR spectroscopy, which revealed two phosphorus environments. Based on previous experiments, the main broad signal between 34.3 and 35.2 ppm was attributed to a polyphosphonate sequence.[47] A much smaller signal (~2% relative intensity) was also apparent between 35.2 and 36.0 ppm, evidence of the enchainment between a lactide and a phosphonate unit. This was later confirmed by the analysis of more random poly(phosphonate-*co*-lactide) copolymers (*vide infra*).

Triblock poly(phosphonate-*b*-lactide-*b*-phosphonate) copolymers could be synthesized in a similar way by using a bifunctional initiator, 1,4-benzenedimethanol, at feed ratios of 100:100:2:1 ($[EtPPn]_0$:$[LA]_0$:$[\mathbf{1}]_0$:$[C_6H_4(CH_2OH)_2]_0$). In this case, a more intense resonance corresponding to

lactide-phosphonate enchainment was observed in the ^{31}P NMR spectrum, as expected from a monomer switch on both sides of the centrally growing polymer (Figure S12).

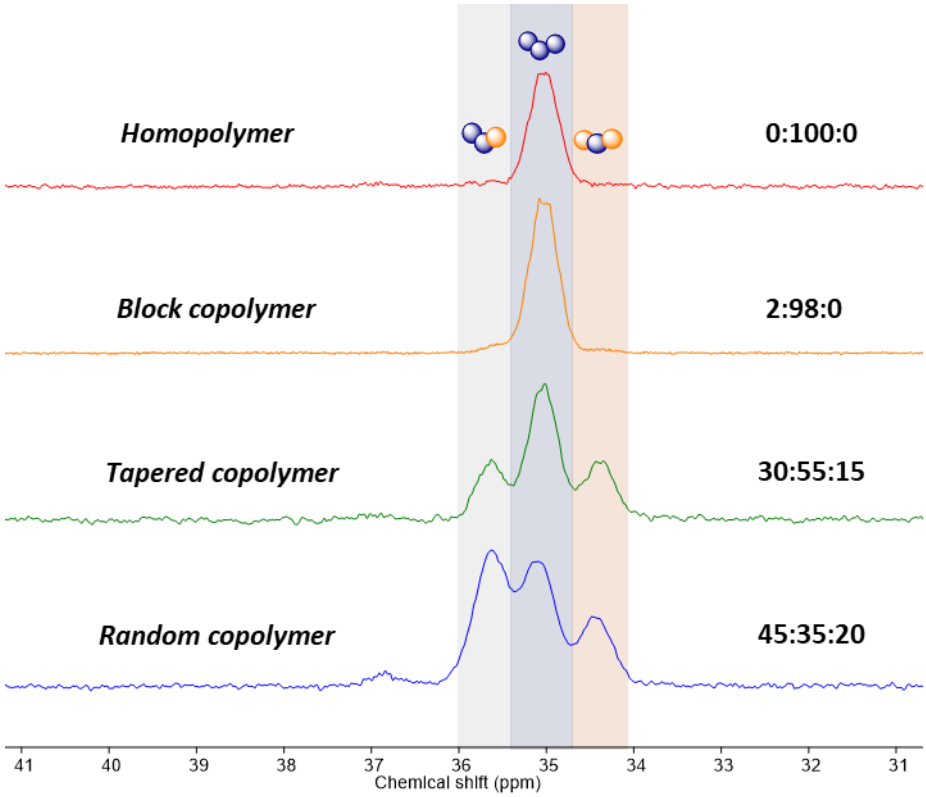

Figure 2. Stacked ^{31}P NMR spectra for copolymers of LA-EtPPn. Triad sequences shown identified as PPL, PPP, and LPL (left to right).

One-pot copolymerization of EtPPn and lactide. Copolymerization was then performed in one pot, from a monomer mixture of rac-LA and EtPPn ($[\text{rac-LA}]_0 = [\text{EtPPn}]_0 = 0.7$ mol L^{-1}), in toluene at 80 °C. Using **1**, complete conversion of EtPPn and high conversion of LA were achieved after 16 h (Table 2, entry 1). The formation of a true copolymer was confirmed by DOSY and unimodal SEC traces ($Đ < 1.27$). It was possible to vary the percentage of EtPPn incorporated into the copolymer (Table 2, Entry 1-4) with a good fit to that of the initial feeds. Molecular weights obtained *via* SEC (most copolymers were soluble in THF) and ^{1}H NMR showed good agreement with expected values (calculated based on monomers conversions). The copolymer microstructure

was further probed *via* ^{31}P NMR spectroscopy, which revealed three phosphorus environments, consistent with the three possible sequence triads involving a central phosphonate linkage: P-**P**-L (or L-**P**-P), P-**P**-P and L-**P**-L (Figure 2). Based on the polyphosphonate and poly(lactide-*b*-phosphonate) polymers prepared previously, the P-P-P and P-P-L triads were identified as the signals at 34.3-35.2 and 35.2-36.0 ppm, respectively. The additional resonance between 33.0 and 34.3 ppm was therefore assigned to L-P-L triad. The ^{31}P NMR for the polymer obtained from Table 2 entry 1 indicated the P-P-P triad was the dominant resonance, albeit with significant P-P-L and L-P-L signals, indicative of a copolymer of a blocky nature. By increasing the LA:EtPPn ratio, the amount of lactide containing triads increased compared to the P-P-P triad, yet without removing it completely, supporting further the blocky nature of the phosphonate linkages in the synthesized copolymers (Table 2 entry 4).

Table 2. Copolymerization of EtPPn with LA to produce copolymers with adjustable microstructure

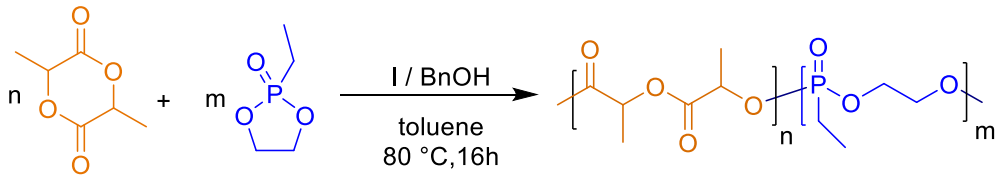

Entry	I	Feed ratio [LA]:[EtPPn]:[I]:[BnOH]	Conv. of LA/EtPPn (%)[f]	EtPPn content in polymer (%)[g]	M_n^{SEC} (kg mol^{-1}) [$Đ$][h]	M_n^{NMR} (kg mol^{-1})[j]	M_n^{theo} (kg mol^{-1})[k]	T_g (°C)	P triads ratios PPL:PPP:LPL
1[a]	**1**	50:50:1:1	75/100	57	15.6 [1.06]	13.3	12.3	–9.7	22:51:27
2[a]	**1**	100:50:1:1	77/98	39	12.5 [1.02]	8.6	18.0	–3.1	28:59:13
3[a]	**1**	100:20.1:1	83/100	19	16.2 [1.27]	16.6	14.8	19.6	28:45:27

4[a]	**1**	100:10.1:1	95/100	10	12.9 [1.23]	11.7	15.2	27.4	44:15:41
5[b]	**1**	50:50.1:1	73/100	58	21.0 [1.12]	9.5	12.2	18.7	21:62:17
6[b]	**1**	100:50:1:1	75/100	40	20.6 [1.06]	20.1	17.6	23.3	29:38:33
7[c]	**1**	50:50:1:1	30/96	76	6.1 [1.31][i]	7.7	8.8	–35.8	8:87:5
8[b]	**2**	50:50:1:1	85/67	45	4.3 [1.10]	8.6	10.5	2.9	30:45:25
9[d]	**2**	50:50:1:1	81/46	35	4.8 [1.18]	8.6	9.4	7.9	32:35:34
10[e]	**2**	50:50:1:1	91/18	17	3.2 [1.10]	7.2	7.9	18.1	40:14:46

[a] $[\text{rac-LA}]_0 = 0.7$ mol L^{-1}, $[\text{EtPPn}]_0$ varies; [b] $[\text{L-LA}]_0 = 0.7$ mol L^{-1}, $[\text{EtPPn}]_0$ varies; [c] $[\text{L-LA}]_0 = [\text{EtPPn}]_0 = 0.35$ mol L^{-1}, at 25 °C for 120h; [d] $[\text{L-LA}]_0 = [\text{EtPPn}]_0 = 0.35$ mol L^{-1}; [e] $[\text{L-LA}]_0 = [\text{EtPPn}]_0 = 0.35$ mol L^{-1}, in CH_2Cl_2 at 25 °C for 16h; [f] Conversions calculated from ^{1}H NMR by relative integration of the side chain CH_2 signals corresponding to EtPPn and poly(EtPPN), and of the methine region of LA and PLA; [g] Calculated from the ratio of polymer units in the crude product; [h] Determined by SEC, carried out in THF at 35 °C; [i] Determined by SEC, carried out in DMF at 60 °C; [j] Calculated from the integration of polymer signals against the BnO- end group; [k] Calculated from conversion of each monomer (M) multiplied by $[M]_0/[I]_0$.

To gain further insight, copolymerization kinetics were monitored *in situ* in toluene-d_8 at 80 °C, and the microstructure of the copolymer evaluated as a function of time, using ^{1}H and ^{31}P NMR spectroscopy (Figure 3a). In these experiments, temperature equilibration, lactide dissolution in toluene, and data acquisition delay means that the first 10 minutes of the reaction cannot be reliably quantified. However, within this period, 70% of EtPPn and 17% of lactide has polymerized, so that a copolymer with a high proportion of P-P-P linkages (66%) is already present at the start of the monitoring. Next, EtPPn continues to be incorporated preferentially into the copolymer: the conversion of individual monomers can be successfully modelled using a pseudo first order kinetics approach,[46] but EtPPn reacts twice as fast compared to L-LA ($k_{\text{obs(EtPPn)}} = 9.0 \times 10^{-3}$ min^{-1}

and $k_{obs(LA)}$= 4.4 × 10^{-3} min^{-1} (Figure S40)). As the conversion of EtPPn plateaus, at 88%, and [EtPPn] decreases, the proportion of PLA linkages in the copolymer increases and lactide polymerization becomes dominant. This results in a gradient copolymer with poly(EtPPn) as the first block, followed by a tapered segment of LA and EtPPn, and finally a PLA homopolymer block.

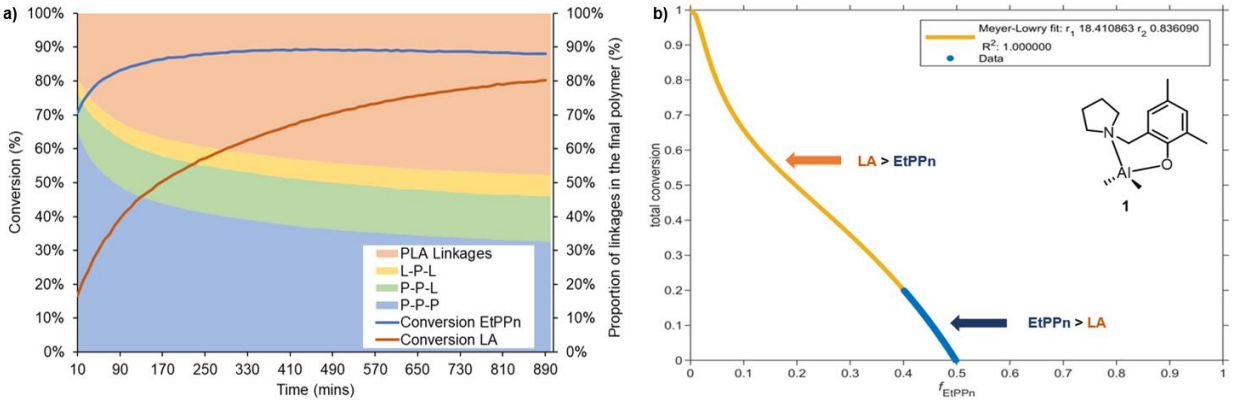

Figure 3. NMR monitored copolymerization of EtPPn and L-LA in toluene-d_8, $[L\text{-}LA]_0 = [EtPPn]_0$ = 0.35 mol L^{-1}, $[L\text{-}LA]_0$:$[EtPPn]_0$:[**1**]$_0$:$[BnOH]_0$ = 50:50:1:1, 80 °C, 16h: a) conversion and microstructure composition calculated from ^{31}P NMR *vs*. time; b) calculation of EtPPn and L-LA reactivity ratios using Meyer-Lowry fits.

DBU (**2**) was also trialed for the one-pot copolymerization of EtPPn and L-LA. Compared to when using **1**, a stark difference was observed in the reactivity of the comonomers and in the microstructure of the resulting copolymers, with lower EtPPn incorporation and more random phosphorus-containing linkages obtained (Table 2 entries 8–10). Under the conditions used previously, initial rate kinetic analysis showed a much faster propagation rate for L-LA (k_{obs}= 6.5 × 10^{-3} min^{-1}) than for EtPPn (k_{obs}= 6.3 × 10^{-4} min^{-1}) (Figure 4a and Figure S30). With low EtPPn conversion (around 25% after 14h) is it likely that this system feature a dispersion of EtPPn throughout the PLLA chain, with an increase in tapering as [EtPPn] exceeds [L-LA]. This yields

a polymer with thermal properties closer to that of PLLA with a glass transition temperature T_g = 18.1 °C, whilst distributing the more biodegradable units throughout.

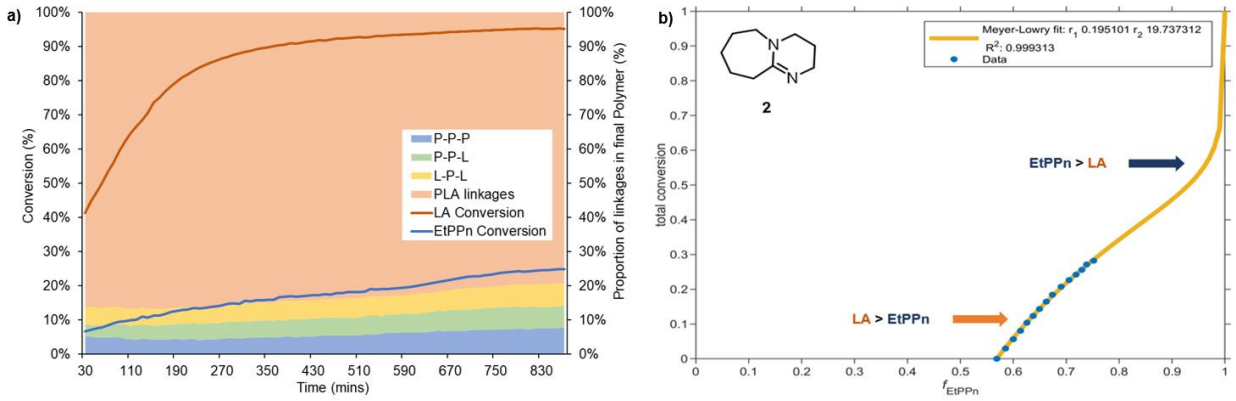

Figure 4. NMR monitored copolymerization of EtPPn and L-LA in toluene-d_8, $[\text{L-LA}]_0 = [\text{EtPPn}]_0$ = 0.35 mol L^{-1}, $[\text{L-LA}]_0:[\text{EtPPn}]_0:[\mathbf{2}]_0:[\text{BnOH}]_0$ = 50:50:1:1, 80 °C, 16h: a) conversion and microstructure composition calculated from ^{31}P NMR *vs*. time; b) calculation of EtPPn and L-LA reactivity ratios using Meyer-Lowry fits.

The reactivity ratios of each monomer (EtPPn = r_1, L-LA = r_2) was calculated from kinetic data and supports the formation of tapered block copolymers with both **1** and **2** ($r_1 >> 1 >> r_2$ and $r_1 << 1 << r_2$, respectively). Using **1**, the high speed of reaction limited the recording of data at low monomer conversions, so that a data fit was applied to the experimental results (Figure S46 and S47). From Meyor-Lowry methodologies, values of r_1 = 18.41 and r_2 = 0.83 are obtained for **1**, while reverse reactivity is seen when **2** is the initiator (r_1 =0.19, r_2 = 19.74) (Figures 3b and 4b).[48] Meyer-Lowry log, Jaacks and Direct Numerical Integration methods agree with these trends, albeit some variations on r values are observed (Figure S50-S57, Table S4 and S5).[48–51] This analysis further confirms that initiator choice has a profound impact on the microstructure of the copolymer.

Temperature sequence for the preparation of block copolymers from a mixture of EtPPn and lactide. The gradient strength of one-pot copolymers was further increased by a sequential temperature protocol. As LA is poorly soluble but EtPPn undergoes rapid ROP in toluene at room temperature, the selectivity for EtPPn should be increased under such copolymerization conditions. A temperature sequence was therefore applied to a copolymerization experiment in toluene-d_8 ($[EtPPn]_0$:$[L\text{-}LA]_0$:$[BnOH]_0$:$[1]_0$ = 50:50:1:1): 2 hours at 25 °C, then 16 hours at 80 °C. The reaction was monitored *in-situ* by ^{1}H and ^{31}P NMR spectroscopy. During the first phase of this protocol, 66% of EtPPn and less than 5% of L-LA conversion reacted, yielding a polymer with almost exclusively (>99%) P-P-P linkages, *i.e.* an almost pure polyphosphonate first block (Figure 5). When the temperature was increased to 80 °C, simultaneous conversion of both monomers was seen, with all possible linkages observed, indicative of statistical copolymerization. As in previous examples, once the conversion of EtPPn reached a plateau, polymerization of L-LA occurred with the formation of a pure PLLA block, without further incorporation or EtPPn.

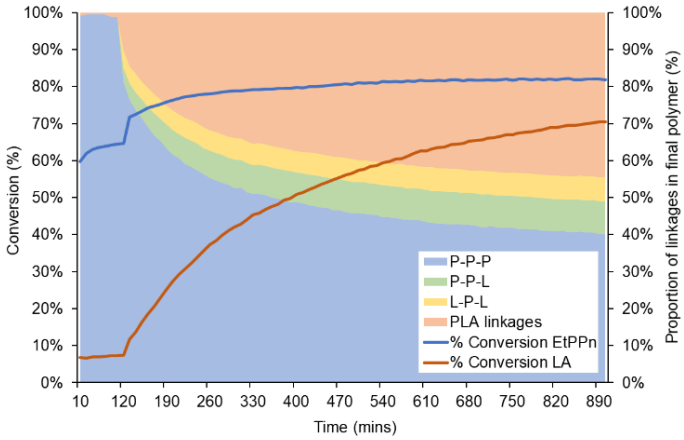

Figure 5. NMR monitored copolymerization of EtPPn and L-LA in toluene-d_8 ($[L\text{-}LA]_0$ = $[EtPPn]_0$ = 0.35 mol L^{-1}, $[L\text{-}LA]_0$:$[EtPPn]_0$:[**1**]$_0$:$[BnOH]_0$ = 50:50:1:1), using the temperature sequence: 1) 25 °C, 2h, 2) 80 °C, 14h. Final copolymer: P triad composition P-P-L:P-P-P:L-P-L = 12:73:15; M_n^{SEC} = 11750 g mol^{-1}, $Đ$ = 1.09.

Increasing the time of the initial 25 °C phase did not increase the conversion of EtPPn or L-LA, whether the reaction was monitored *in-situ* or via sampling from a stirred solution (Figures S43 and S44).

Whilst pure blocks are not accessible yet with this methodology, a significant reduction in the statistical enchainment of monomers (P triads ratios P-P-L:P-P-P:L-P-L = 12:73:15 in comparison to 21:61:17 (Table 2 entry 5)) shows the potential of temperature sequencing to exacerbate differences in reactivity ratios and lead to clean block poly(phosphonate-*co*-lactide) copolymers in one-pot. Through the same temperature sequencing, but at higher monomer concentrations of 3.4 mol L^{-1}, a further reduction in tapering was achieved (P triads ratios P-P-L:P-P-P:L-P-L = 9:84:7), whilst also granting a significant increase in polymerization rate (Entry 10, Table S3).

Thermal analysis. DSC analysis of poly(phosphonate-*co*-lactide) copolymers synthesized with **1** showed a negative correlation between the molar fraction of EtPPn incorporated and the glass transition temperature. The Al initiator thus give access to copolymers with a range of glass transitions between that of the homopolymers (Figure 6). This behavior is expected for random copolymer systems as expressed in the Fox equation.[52] A similar trend has been observed with the copolymerization of ^{cy}HexPPn and ^{i}PrPPn.[43] Copolymers produced by temperature sequencing also yielded copolymers with only one transition (Figures S61 and S62). Only copolymers from sequential addition exhibited two distinct thermal transitions at 63.9 and –48.0 °C, indicating that monomer misinsertion is then low enough to form polymer blocks capable of phase separation.

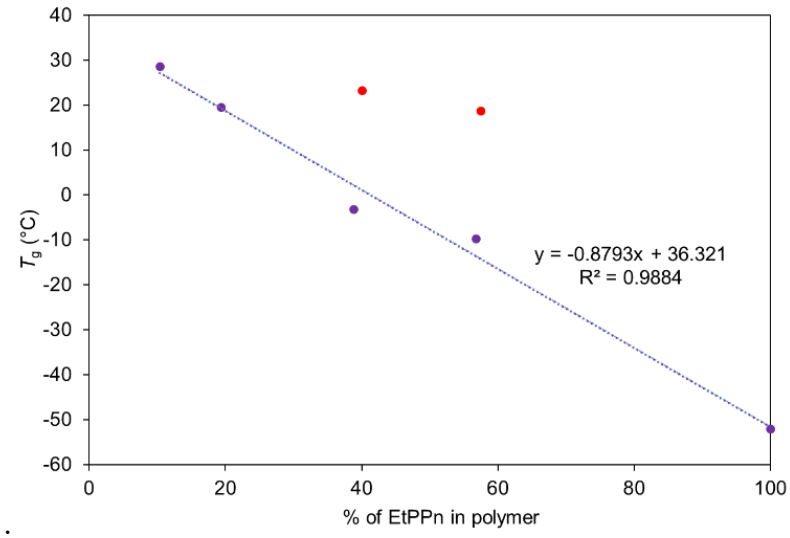

Figure 6. T_g of poly(phosphonate-*co*-lactide) tapered block copolymers depending on EtPPn content (type of lactide unit: ● rac-LA, ● L-LA).

Thermal gravimetric analysis (TGA) showed poly(phosphonate-*co*-lactide) copolymers to degrade within a wide temperature range (130–350 °C), with degradation profiles eluding to their microstructure (Figures 6 and S61–68). Tapered block copolymers thus showed only one degradation step, closer to that of pure P(EtPPn) or PLA, depending on the use of initiator **1** or **2** respectively. Block polymers synthesized from sequential addition displayed two distinct degradation steps, with derivative maxima at 227 °C and 336 °C, indicative of P(EtPPn) and PLLA blocks respectively, with an initial onset at 138 °C (Figure S65). Triblock poly(phosphonate-*b*-lactide-*b*-phosphonate) copolymer showed similar features but proved more stable, with degradation derivative maxima at 269°C (corresponding to 63% mass loss) and 352°C (further 37% mass loss) (Figure S68). This is likely a result of the greater degree of polymerization in this system. For block copolymers, peak deconvolution also yielded an associated % mass loss for each degradation step (*e.g.* 63 and 37 % mass loss in the case of the triblock), which could be linked to the content of each monomer in the copolymer (60% of EtPPn units and 39% of L-LA units). This

aligned well with polymer ratios (EtPPn:L-LA = 58:42) calculated through NMR spectroscopic analysis of the purified sample, providing an additional method for the analysis of block copolymers.

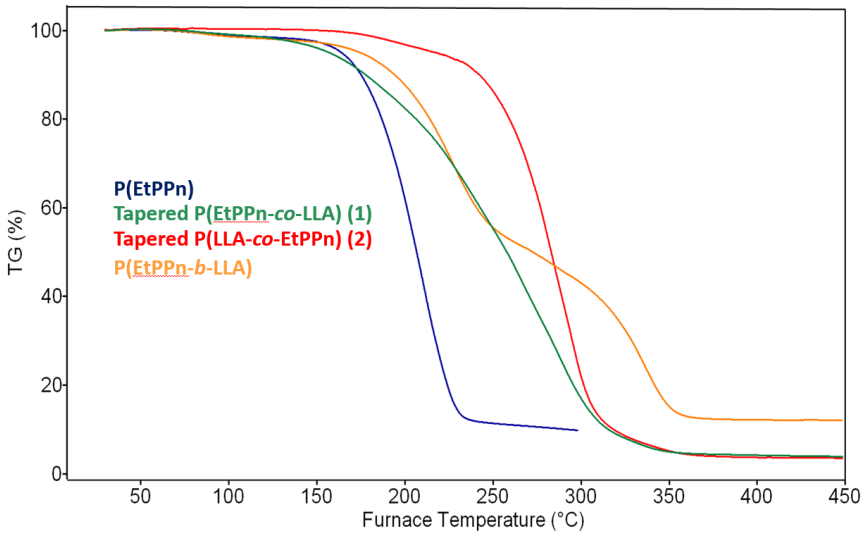

Figure 7. TGA analysis of poly(phosphonate-*co*-lactide) copolymers of various microstructure. Tapered P(EtPPn-*co*-LLA) (**1**) was made using **1**, tapered P(LLA-co-EtPPn) (2) was made using **2**, see details in ESI (Figures S61-68).

Conclusion

Copolymers of a cyclic phosphonate (2-ethyl-2-oxo-1,3,2-dioxaphospholane) and lactide have been prepared for the first time. We were able to control the microstructure of the copolymer (determined by ^{1}H and ^{31}P NMR spectroscopy), via judicious choice of initiator (Al complex (**1**) or DBU (**2**), in combination with benzyl alcohol), and via the polymerization conditions (sequential addition or one-pot copolymerization, concentration, temperature). Block copolymers were obtained by sequential monomer addition and tapered block copolymers were obtained by one-pot copolymerization. Interestingly, the choice of the catalyst inverted the reactivity ratios of the comonomers. The degree of tapering could also be reduced using a temperature sequence

protocol, providing a route to one-pot block copolymer synthesis and an additional handle to tune the properties of the resulting poly(phosphonate-co-esters). Such amphiphilic copolymers with adjustable thermal properties are interesting candidates for future applications in drug delivery or materials science, including because they are likely to also exhibit tunable degradation patterns. Future work will focus on investigating the hydrolytic degradation profiles of the copolymers.

ASSOCIATED CONTENT

Supporting Information. Experimental details; NMR, SEC, TGA, DSC and MALDI-ToF data for copolymers; kinetic data for copolymerization experiments and reactivity ratios calculations. The Supporting Information is available free of charge on the ACS Publications website.

AUTHOR INFORMATION

Corresponding Authors

*AB: a.buchard@bath.ac.uk; MDJ: mj205@bath.ac.uk; FRW: wurm@mpip-mainz.mpg.de.

Author Contributions

The manuscript was written through contributions of all authors. All authors have given approval to the final version of the manuscript.

Funding Sources

We thank the EPSRC and University of Bath for funding a studentship for JB. AB acknowledges Roger and Sue Whorrod (fellowship) and the Royal Society (UF/160021 fellowship).

Notes

The authors declare no competing financial interests.

ACKNOWLEDGMENT

Analytical facilities were provided through the Chemical Characterization and Analysis Facility (CCAF) at the University of Bath and the Max Planck Institute for Polymer Research.

REFERENCES

(1) Nguyen, H. T. H.; Qi, P.; Rostagno, M.; Feteha, A.; Miller, S. A. The Quest for High Glass Transition Temperature Bioplastics. *J. Mater. Chem. A* **2018**, *6*, 9298–9331.

(2) Sin, L. T.; Rahmat, A.; Rahman, W. A. W. A. *Polylactic Acid: PLA Biopolymer Technology and Applications*; William Andrew, 2012.

(3) Yu, S.; Xiang, H.; Zhou, J.; Zhu, M. Preparation and Characterization of Fire Resistant PLA Fibers with Phosphorus Flame Retardant. *Fibers Polym.* **2017**, *18* (6), 1098–1105.

(4) European Bioplastics; Institute for Bioplastics and Biocomposites. *Bioplastics Market Data 2017*; 2017.

(5) Dijkstra, P. J.; Du, H.; Feijen, J. Single Site Catalysts for Stereoselective Ring-Opening Polymerization of Lactides. *Polym. Chem.* **2011**, *2* (3), 520–527.

(6) Rudeekit, Y.; Numnoi, J.; Tajan, M.; Chaiwutthinan, P.; Leejarkpai, T. Determining Biodegradability of Polylactic Acid under Different Environments. *J. Met. Mater. Miner.* **2008**, *18* (2), 83–87.

(7) Haider, T.; Völker, C.; Kramm, J.; Landfester, K.; Wurm, F. R. Plastics of the Future? The Impact of Biodegradable Polymers on the Environment and on Society. *Angew. Chem Int. Ed.* **2019**, *58*, 50-62.

(8) Rocca-Smith, J. R.; Whyte, O.; Brachais, C. H.; Champion, D.; Piasente, F.; Marcuzzo, E.; Sensidoni, A.; Debeaufort, F.; Karbowiak, T. Beyond Biodegradability of Poly(Lactic Acid): Physical and Chemical Stability in Humid Environments. *ACS Sustain. Chem. Eng.* **2017**, *5* (3), 2751–2762.

(9) Muller, J.; González-Martínez, C.; Chiralt, A. Combination Of Poly(Lactic) Acid and Starch for Biodegradable Food Packaging. *Materials* **2017**, *10* (8), 1–22.

(10) Yemisci, F.; Aytac, A. Compatibilization of Poly(Lactic Acid)/Polycarbonate Blends by Different Coupling Agents. *Fibers Polym.* **2017**, *18* (8), 1445–1451.

(11) Pepper, K. J.; Masson, T.; De Focatiis, D.; Howdle, S. M. Can a Combination of Poly(Ethylene Glycol) and Dense Phase Carbon Dioxide Improve Processing of Polylactide? A High Pressure Rheology Investigation. *J. Supercrit. Fluids* **2018**, *133*, 343–348.

(12) Han, W.; Ren, J.; Xuan, H.; Ge, L. Controllable Degradation Rates, Antibacterial, Free-Standing and Highly Transparent Films Based on Polylactic Acid and Chitosan. *Colloids Surfaces A Physicochem. Eng. Asp.* **2018**, *541*, 128–136.

(13) Chaiwutthinan, P.; Pimpan, V.; Chuayjuljit, S.; Leejarkpai, T. Biodegradable Plastics Prepared from Poly(Lactic Acid), Poly(Butylene Succinate) and Microcrystalline Cellulose Extracted from Waste-Cotton Fabric with a Chain Extender. *J. Polym. Environ.* **2015**, *23* (1), 114–125.

(14) Suthapakti, K.; Molloy, R.; Punyodom, W.; Nalampang, K.; Leejarkpai, T.; Topham, P. D.; Tighe, B. J. Biodegradable Compatibilized Poly(l-Lactide)/Thermoplastic Polyurethane Blends: Design, Preparation and Property Testing. *J. Polym. Environ.* **2017**, *26* (5), 1–13.

(15) Martin, R. T.; Camargo, L. P.; Miller, S. A. Marine-Degradable Polylactic Acid. *Green Chem.* **2014**, *16* (4), 1768–1773.

(16) Nguyen, H. T. H.; Short, G. N.; Qi, P.; Miller, S. A. Copolymerization of Lactones and Bioaromatics via Concurrent Ring-Opening Polymerization/Polycondensation. *Green Chem.* **2017**, *19* (8), 1877–1888.

(17) Marsico, F.; Wagner, M.; Landfester, K.; Wurm, F. R. Unsaturated Polyphosphoesters via Acyclic Diene Metathesis Polymerization. *Macromolecules* **2012**, *45* (21), 8511–8518.

(18) Steinbach, T.; Alexandrino, E. M.; Wurm, F. R. Unsaturated Poly(Phosphoester)s via Ring-Opening Metathesis Polymerization. *Polym. Chem.* **2013**, *4* (13), 3800–3806.

(19) Bauer, K. N.; Liu, L.; Andrienko, D.; Wagner, M.; Macdonald, E. K.; Shaver, M. P.; Wurm, F. R. Polymerizing Phostones: A Fast Way to In-Chain Poly(Phosphonate)s with Adjustable Hydrophilicity. *Macromolecules* **2018**, *51* (4), 1272–1279.

(20) Bauer, K. N.; Tee, H. T.; Velencoso, M. M.; Wurm, F. R. Main-Chain Poly(Phosphoester)s: History, Syntheses, Degradation, Bio-and Flame-Retardant Applications. *Prog. Polym. Sci.* **2017**, *73*, 61–122.

(21) Kalużyński, K.; Libiszowski, J.; Penczek, S. A New Class of Synthetic Polyelectrolytes. Acidic Polyesters of Phosphoric Acid (Poly(Hydroxyalkylene Phosphates)). *Macromolecules* **1976**, *9* (2), 365–367.

(22) Klosiński, P.; Penczek, S. Synthesis of Models of Teichoic Acids by Ring-Opening Polymerization. *Macromolecules* **1983**, *16* (2), 316–320.

(23) *Novel Fire Retardant Polymers and Composite Materials*; Wang, D. Y., Ed.; Elsevier Science, 2016.

(24) Velencoso, M. M.; Battig, A.; Markwart, J. C.; Schartel, B.; Wurm, F. R. Molecular Firefighting - How Modern Phosphorus Chemistry Can Help Solve the Flame Retardancy Task. *Angew. Chem. Int. Ed.* **2018**, *57*, 10450–10467.

(25) Tsao, Y. Y. T.; Wooley, K. L. Synthetic, Functional Thymidine-Derived Polydeoxyribonucleotide Analogues from a Six-Membered Cyclic Phosphoester. *J. Am. Chem. Soc.* **2017**, *139* (15), 5467–5473.

(26) Tsao, Y. Y. T.; Smith, T. H.; Wooley, K. L. Regioisomeric Preference in Ring-Opening Polymerization of 3′,5′-Cyclic Phosphoesters of Functional Thymidine DNA Analogues. *ACS Macro Lett.* **2018**, *7* (2), 153–158.

(27) Pratt, R. C.; Lohmeijer, B. G. G.; Long, D. A.; Lundberg, P. N. P.; Dove, A. P.; Li, H.; Wade, C. G.; Waymouth, R. M.; Hedrick, J. L. Exploration, Optimization, and Application of Supramolecular Thiourea-Amine Catalysts for the Synthesis of Lactide (Co)Polymers. *Macromolecules* **2006**, *39* (23), 7863–7871.

(28) Lohmeijer, B. G. G.; Pratt, R. C.; Leibfarth, F.; Logan, J. W.; Long, D. A.; Dove, A. P.; Nederberg, F.; Choi, J.; Wade, C.; Waymouth, R. M.; et al. Guanidine and Amidine Organocatalysts for Ring-Opening Polymerization of Cyclic Esters. *Macromolecules* **2006**, *39* (25), 8574–8583.

(29) Kiesewetter, M. K.; Shin, E. J.; Hedrick, J. L.; Waymouth, R. M. Organocatalysis: Opportunities and Challenges for Polymer Synthesis. *Macromolecules* **2010**, *43* (5), 2093–2107.

(30) Clément, B.; Grignard, B.; Koole, L.; Jéroîme, C.; Lecomte, P. Metal-Free Strategies for the Synthesis of Functional and Well-Defined Polyphosphoesters. *Macromolecules* **2012**, *45* (11), 4476–4486.

(31) Darensbourg, D. J.; Choi, W.; Ganguly, P.; Richers, C. P. Biometal Derivatives as Catalysts for the Ring-Opening Polymerization of Trimethylene Carbonate. Optimization of the Ca(II) Salen Catalyst System. *Macromolecules* **2006**, *39* (13), 4374–4379.

(32) Yasuda, H.; Sumitani, M.; Nakamura, A. Novel Synthesis of Acidic Polyesters of Phosphoric Acid by Thermal Elimination of Isobutylene from Poly(Alkylene Tert-Butyl Phosphates). *Macromolecules* **1981**, *14* (2), 458–460.

(33) Xiao, C. S.; Wang, Y. C.; Du, J. Z.; Chen, X. S.; Wang, J. Kinetics and Mechanism of 2-Ethoxy-2-Oxo-1,3,2-Dioxaphospholane Polymerization Initiated by Stannous Octoate. *Macromolecules* **2006**, *39* (20), 6825–6831.

(34) Iwasaki, Y.; Yamaguchi, E. Synthesis of Well-Defined Thermoresponsive Polyphosphoester Macroinitiators Using Organocatalysts. *Macromolecules* **2010**, *43* (6), 2664–2666.

(35) Stukenbroeker, T. S.; Solis-Ibarra, D.; Waymouth, R. M. Synthesis and Topological Trapping of Cyclic Poly(Alkylene Phosphates). *Macromolecules* **2014**, *47* (23), 8224–8230.

(36) Nifant'ev, I. E.; Shlyakhtin, A. V.; Bagrov, V. V.; Komarov, P. D.; Kosarev, M. A.; Tavtorkin, A. N.; Minyaev, M. E.; Roznyatovsky, V. A.; Ivchenko, P. V. Controlled Ring-Opening Polymerisation of Cyclic Phosphates, Phosphonates and Phosphoramidates Catalysed by Heteroleptic BHT-Alkoxy Magnesium Complexes. *Polym. Chem.* **2017**, *8* (44), 6806–6816.

(37) Lim, Y. H.; Tiemann, K. M.; Heo, G. S.; Wagers, P. O.; Rezenom, Y. H.; Zhang, S.; Zhang, F.; Youngs, W. J.; Hunstad, D. A.; Wooley, K. L. Preparation and in Vitro Antimicrobial Activity of Silver-Bearing Degradable Polymeric Nanoparticles of Polyphosphoester-Block-Poly(l-Lactide). *ACS Nano* **2015**, *9* (2), 1995–2008.

(38) Yang, X.-Z.; Sun, T.-M.; Dou, S.; Wu, J.; Wang, Y.-C.; Wang, J. Block Copolymer of Polyphosphoester and Poly(l -Lactic Acid) Modified Surface for Enhancing Osteoblast Adhesion, Proliferation, and Function. *Biomacromolecules* **2009**, *10* (8), 2213–2220.

(39) Lim, Y. H.; Heo, G. S.; Cho, S.; Wooley, K. L. Construction of a Reactive Diblock Copolymer, Polyphosphoester- Block -Poly(l -Lactide), as a Versatile Framework for Functional Materials That Are Capable of Full Degradation and Nanoscopic Assembly Formation. *ACS Macro Lett.* **2013**, *2* (9), 785–789.

(40) Borguet, Y. P.; Khan, S.; Noel, A.; Gunsten, S. P.; Brody, S. L.; Elsabahy, M.; Wooley, K. L. Development of Fully Degradable Phosphonium-Functionalized Amphiphilic Diblock Copolymers for Nucleic Acids Delivery. *Biomacromolecules* **2018**, *19* (4), 1212–1222.

(41) Wolf, T.; Steinbach, T.; Wurm, F. R. A Library of Well-Defined and Water-Soluble Poly(Alkyl Phosphonate)s with Adjustable Hydrolysis. *Macromolecules* **2015**, *48* (12), 3853–3863.

(42) Wolf, T.; Rheinberger, T.; Wurm, F. R. Thermoresponsive Coacervate Formation of Random Poly(Phosphonate) Terpolymers. *Eur. Polym. J.* **2017**, *95*, 756–765.

(43) Wolf, T.; Naß, J.; Wurm, F. R. Cyclohexyl-Substituted Poly(Phosphonate)-Copolymers with Adjustable Glass Transition Temperatures. *Polym. Chem.* **2016**, *7* (17), 2934–2937.

(44) Wolf, T.; Rheinberger, T.; Simon, J.; Wurm, F. R. Reversible Self-Assembly of Degradable Polymersomes with Upper Critical Solution Temperature in Water. *J. Am. Chem. Soc.* **2017**, *139* (32), 11064–11072.

(45) Macdonald, E. K.; Shaver, M. P. An Expanded Range of Catalysts for Synthesising Biodegradable Polyphosphonates. *Green Mater.* **2016**, *4*, 81–88.

(46) Beament, J.; Mahon, M. F.; Buchard, A.; Jones, M. D. Aluminum Complexes of Monopyrrolidine Ligands for the Controlled Ring-Opening Polymerization of Lactide. *Organometallics* **2018**, *37*, 1719–1724.

(47) Steinbach, T.; Ritz, S.; Wurm, F. R. Water-Soluble Poly(Phosphonate)s via Living Ring-Opening Polymerization. *ACS Macro Lett.* **2014**, *3* (3), 244–248.

(48) Patino-Leal, H.; Reilly, P. M.; O'Driscoll, K. F. On the Estimation of Reactivity Ratios. *J. Polym. Sci. Polym. Lett. Ed.* **1980**, *18* (3), 219–227.

(49) Kazemi, N.; Duever, T. A.; Penlidis, A. Reactivity Ratio Estimation from Cumulative Copolymer Composition Data. *Macromol. React. Eng.* **2011**, *5* (9–10), 385–403.

(50) Hauch, E.; Zhou, X.; Duever, T. A.; Penlidis, A. Estimating Reactivity Ratios from Triad Fraction Data. *Macromol. Symp.* **2008**, *271* (1), 48–63.

(51) Jaacks, V. A Novel Method of Determination of Reactivity Ratios in Binary and Ternary Copolymerizations. *Macromol. Chem. Phys.* **1972**, *161* (1), 161–172.

(52) Brostow, W.; Chiu, R.; Kalogeras, I. M.; Vassilikou-Dova, A. Prediction of Glass Transition Temperatures: Binary Blends and Copolymers. *Mater. Lett.* **2008**, *62* (17–18), 3152–3155.